Laboratory measurements of charge separation in low liquid water content conditions and low impact velocity

Eldo E. Ávila,[1] Rafael A. Lighezzolo,[1] Nesvit E. Castellano,[1] Rodolfo G. Pereyra,[1] and Rodrigo E. Bürgesser[1]

Received 2 January 2013; revised 31 May 2013; accepted 4 June 2013.

[1] A laboratory investigation of the electric charge separated in collisions between vapor-grown ice crystals and a target growing by riming is presented in this work, with the goal of studying the performance of the noninductive mechanism under microphysical conditions similar to some of those which occur in the stratiform regions of the mesoscale convective systems. A series of experiments were conducted by using a target of 2 mm in diameter, for ambient temperatures between −7°C and −13°C, effective liquid water content between 0.05 and 0.5 g m^{-3}, and air speeds between 1 and 3 m s^{-1}. Charge diagrams of the sign of the electric charge transfer on the rimer as a function of the ambient temperature and the effective liquid water content for each velocity are presented. The results show that the riming target charges positive for temperatures above −10°C. For temperatures below −10°C, the charging is positive for high liquid water content and negative for low liquid water content. The magnitude of the charge transfer per collision under the studied conditions ranges from 0.01 to 0.2 fC. The implications of these results to the electrification processes are discussed.

Citation: Ávila, E. E., R. A. Lighezzolo, N. E. Castellano, R. G. Pereyra, and R. E. Bürgesser (2013), Laboratory measurements of charge separation in low liquid water content conditions and low impact velocity, *J. Geophys. Res. Atmos.*, *118*, doi:10.1002/jgrd.50555.

1. Introduction

[2] The electrical structure of the mesoscale convective systems (MCSs) has been unraveled with balloon soundings of electric field in numerous field observations. Based on a one-dimensional analysis of Poisson's equation, it is possible to estimate the vertical distribution of the electric charge. The results show that the electric fields and the charge densities in the stratiform regions are of the same order of magnitude as those observed in convective cores [*Schuur et al*., 1991; *Marshall and Rust*, 1993; *Stolzenburg et al*., 1994, 1998]. A typical MCS stratiform cloud covers 2×10^3 to 2×10^4 km^2, lasts between 2 and 12 h, and can separate a large amount of electric charge estimated at 2×10^4 C, which is substantially greater than the values associated with ordinary thunderclouds. In general, the results show a complex electrical structure in terms of the number of significant charge regions inside the cloud. Usually, dense charge layers near the 0°C isotherm are observed. Different balloon soundings show that the charge of both polarities can exist near the melting zone [*Marshall and Rust*, 1993; *Stolzenburg and Marshall*, 2008]. The existence of the dense charge layer near the melting level has been discussed by *Stolzenburg et al*. [1994] and *Shepherd et al*. [1996] and they suggested that a melting-charging mechanism may be operative within this region. *Shepherd et al*. [1996] found evidence that high electric field and charge densities near the melting level are linked to the presence of the radar bright band. This bright band is associated with the melting of hydrometeors [*Fabry and Zawadzki*, 1995], on which charges could be induced prior to their breaking apart or shedding.

[3] Many results have suggested that sprites and other transient luminous events commonly occur above the stratiform region of the MCSs [*Boccippio et al*., 1995; *Lyons*, 1996]. In particular, *Williams* [1998] suggested that the positive cloud-to-ground discharges from these regions are associated with the triggering of sprites in the upper atmosphere.

[4] In situ measurements revealed a complex microphysical structure of the MCS stratiform region containing a large concentration of frozen droplets of few tens of microns, small ice crystals, and crystals with dendritic growth, aggregates of dendrites, and a wide variety of particle habits, including lightly rimed columns, needles, and graupel with sizes that ranged from 1 to 3 mm [*Schuur and Rutledge*, 2000]. The presence of some rimed particles and small graupel suggests the presence of supercooled cloud water droplets, mainly in the mesoscale updraft region. *Schuur and Rutledge* [2000] reported measurements of supercooled liquid water content (LWC) that ranged from 0.1 to 0.5 g m^{-3} for the −16°C to −8°C layer, while *Willis and Heymsfield* [1989] reported the presence of a small amount of liquid water at temperatures between −5°C and −2°C. The scarcity of measurements of supercooled liquid water content in the stratiform regions is a consequence of the difficulty of measuring this variable in

[1]FaMAF, Universidad Nacional de Córdoba, IFEG-CONICET, Córdoba, Argentina.

Corresponding author: E. E. Ávila, Facultad de Matemática, Astronomía y Física, Universidad Nacional de Córdoba, IFEG-CONICET, Ciudad Universitaria, 5000 Córdoba, Argentina. (avila@famaf.unc.edu.ar)

2169-897X/13/10.1002/jgrd.50555

warm, low liquid water regions with large aggregates present in the cloud.

[5] The results from many laboratory studies suggest that the noninductive collisional charging of ice crystals and graupel may be able to account for the charge separation in the updraft regions [e.g., *Reynolds et al*., 1957; *Takahashi*, 1978; *Jayaratne et al*., 1983; *Brooks et al*., 1997; *Saunders and Peck*, 1998; *Saunders et al*., 1991, 1999, 2001, 2004; *Pereyra et al*., 2000; *Ávila and Pereyra*, 2000]. This charging mechanism allows large and small ice particles to obtain an opposite polarity charge, and then, the particle separation due to fall speed differences can lead to the charge structure observed in the convective regions of the clouds. Besides, *Williams and Yair* [2006] proposed that the noninductive process is capable of explaining macroscopic features of the stratiform region of the MCS.

[6] In general, most of the laboratory studies of charge separation during the ice crystal-graupel collisions have been carried out in conditions similar to those found in the convective regions of thunderstorms (simulated graupel with sizes 4 mm in diameter, or impact velocities $> 3\,\mathrm{m\,s^{-1}}$, or liquid water contents $> 0.5\,\mathrm{g\,m^{-3}}$). There are few studies about graupel charging by collisions with ice crystals under conditions similar to those found in the stratiform regions of the MCS [*Jayaratne et al*., 1983; *Saunders et al*., 1991; *Prakash and Kumar*, 2010]. However, in these studies, not all the variables were within the characteristic ranges of the stratiform regions. For example, *Jayaratne et al*. [1983] and *Saunders et al*. [1991] found that a rimed rod target of 5 mm in diameter charged positively at temperatures above −10°C, $\mathrm{LWC} > 0.2\,\mathrm{g\,m^{-3}}$, and an impact velocity of $3\,\mathrm{m\,s^{-1}}$ and negatively at $\mathrm{LWC} < 0.2\,\mathrm{g\,m^{-3}}$. On the other hand, *Jayaratne et al*. [1983] measured the graupel charging as a function of the impact velocity for speeds between 1 and 3 m $\mathrm{s^{-1}}$. The measurements were performed with the rod target of 5 mm in diameter at a temperature of −11°C and $\mathrm{LWC} = 1\,\mathrm{g\,m^{-3}}$. They found that under these conditions, the rime charged positively, and the magnitude of the charge transfer per event varied between 0.01 and 0.5 fC. In a recent paper, *Prakash and Kumar* [2010] reported the sign charge diagram of a simulated graupel during the ice crystal-graupel collision as a function of temperature (T) and rime accretion rate. The rime accretion rate is equal to the effective liquid water content (EW) times the impact velocity (V). The graupel was grown on a target of 4 mm in diameter at a constant impact velocity of $2.2\,\mathrm{m\,s^{-1}}$, and the temperature was varied between −6°C and −26°C. They found that the graupel charge was positive in the temperature range of −7°C to −12°C. Both negative and positive graupel charging were observed in the temperature range of −17°C to −21°C. Predominant positive charging of the graupel was observed in the temperature region below−21°C. Considering the values of the LWC in the stratiform regions of the MCS, it is possible to observe that these authors have worked with very low liquid water concentration. In fact, they worked with $\mathrm{EW} < 0.05\,\mathrm{g\,m^{-3}}$, which is 1 order of magnitude below the typical EW found in this kind of clouds.

[7] Since the typical microphysical conditions usually found in the stratiform regions of the MCS have not been satisfactorily fulfilled in previous laboratory studies of charge separation during ice crystal-graupel collisions (graupel sizes, velocities, and LWCs were not always in the appropriate ranges), in this paper, we work under laboratory conditions that better resemble the stratiform cloud conditions than those of the previous studies. Thus, the magnitude and sign of the average charge transferred during ice crystal-graupel collisions was determined for a simulated graupel of 2 mm in diameter, impact velocities between 1 and $3\,\mathrm{m\,s^{-1}}$, and effective liquid water content between 0.05 and $0.5\,\mathrm{g\,m^{-3}}$. The goal of this work is to characterize the performance and relevance that the noninductive mechanism may have in the electrification processes in the limited region of the mesoscale updraft region of the MCSs.

2. Experiments

[8] The cloud chamber used in this study consists of a single chamber with a height of 1.8 m and side dimensions of $0.6 \times 0.9\,\mathrm{m^2}$, located inside a cold room. Figure 1 shows the general layout of the apparatus. The device is based on the arrangement used by *Pereyra et al*. [2000], *Bürgesser et al*. [2006], *Pereyra et al*. [2008], and *Lighezzolo et al*. [2010], with some modifications which are described in detail below.

[9] The water droplets were generated by vapor condensation from a boiler located inside the cloud chamber. Ice crystals were nucleated in the supercooled droplet cloud by cooling a local volume of the droplet cloud with a rapid expansion of air from compressed air inside a syringe (the original volume was ~6 mL), after which the ice crystals grew at the expense of the water droplets through the Bergeron process (deposition). The cloud input was maintained to provide a mixed-phase cloud.

[10] The wind tunnel is a vertical cylindrical tube with a section of 10 cm in diameter connected to an air pump placed outside the cold room. The speed of the air (V) inside the tunnel was controlled by adjusting the power to the air pump and measured by an anemometer with an accuracy of $\pm 0.1\,\mathrm{m\,s^{-1}}$. The measurements were conducted at velocities between 1 and 3 m $\mathrm{s^{-1}}$. According to *Locatelli and Hobbs* [1974], the range of velocities used in this work is representative of the fall velocities of graupel particles with a maximum dimension between 1 and 4 mm.

[11] Riming occurs on a collector in a form of network, constituted by brass wires of 2 mm in diameter. This target is placed across the wind tunnel and connected to a sensitive current amplifier whose output current (I) was a measure of ice crystal charging events associated with collision and separation from the target. Figure 2 shows a picture of the rimed target. The area of the gap between the wires is approximately $15 \times 15\,\mathrm{mm^2}$; this area is large enough in order to consider that the flow pattern around the target is mainly produced by the wire diameter. The network-type collector was used instead of the typical single rod target used in the previous works [*Takahashi*, 1978; *Jayaratne et al*., 1983; *Saunders et al*., 1991, 2004, 2006; *Pereyra and Ávila*, 2002; etc.] because of the low-magnitude charging current produced in these kinds of experiments as a consequence of the low-speed collisions. Thus, with this device, it was possible to increase sufficiently the ice crystals impacting area on the target in order to get detectable charging currents. The velocity distribution along the mesh was fairly uniform within the anemometer accuracy, except close to the tunnel wall, where the speed decreases between 10% and 20%. This effect was not considered in the determination of the flow velocity.

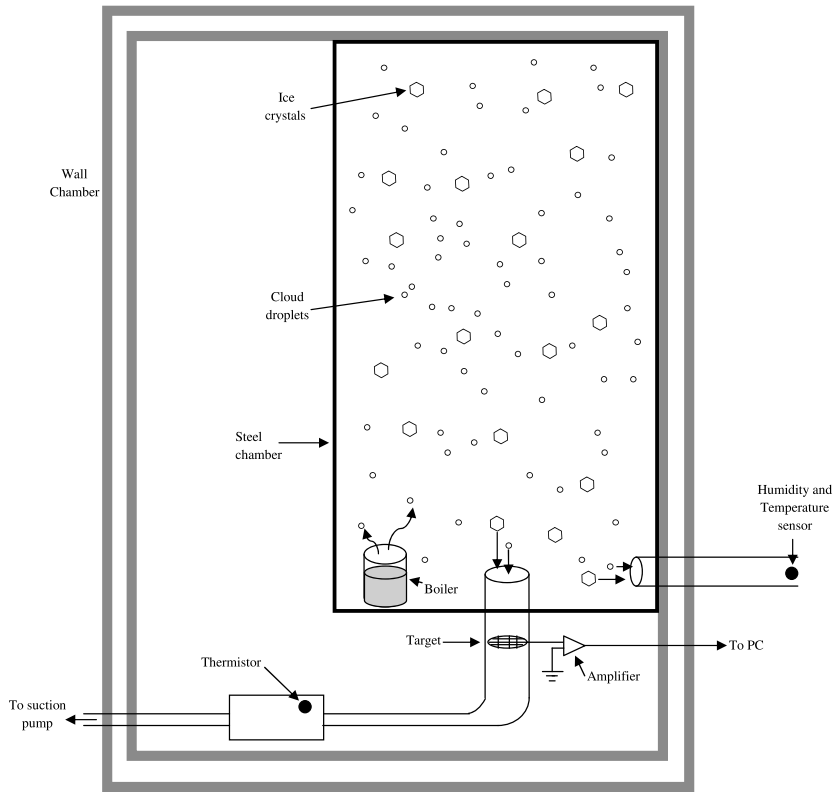

Figure 1. Sketch of the experimental chamber used for laboratory studies.

[12] The ambient temperature (T) was determined by a thermistor located in the lower part of the wind tunnel and was sensed as a function of time during the run. The variation of T during the measurement was included in the error term, and it was typically $< 2°C$. The effective liquid water content (EW) was experimentally determined by weighing the deposit of rime collected on the target during the run; the time interval of the EW determination was between 40 and 50 s; the uncertainty in the measured EW was typically about 30%. In order to determine the LWC from EW, it is necessary to estimate the collection efficiency coefficient (Ce), which depends on the impact velocity, the sizes of the collector, and the droplets (LWC = EW/Ce). The Ce can take low values ($Ce \ll 1$), particularly for low velocities and small droplets, which makes some of the EW measured in this work bigger than the maximum LWC values in the stratiform regions. The total water content (TWC) was also experimentally determined by using a psychrometric method [*Jayaratne et al.*, 1983]. A sample of the air from the cloud chamber was drawn out at a steady flow rate through a heated metal tube so that the condensed water was completely evaporated. The relative humidity and temperature of this air was measured by using a psychrometer (TESTO 435-4), and the TWC was obtained by subtracting the corresponding weight of the water vapor from the total

Figure 2. Picture of the rimed target. The wires of the network are 2 mm in diameter.

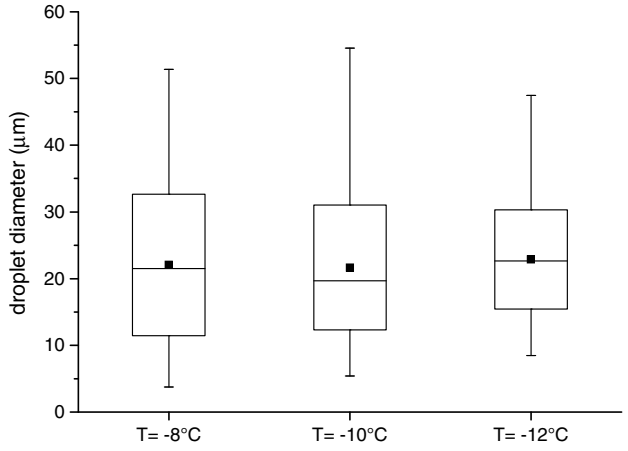

Figure 3. Statistical analyses as box charts for the cloud droplet sizes for $T = -8°C, -10°C$, and $-12°C$. The squares and horizontal bars inside the boxes indicate the mean and median droplet diameters, respectively. The boxes indicate the standard deviation, and the small dashes indicate the minimum and maximum droplet diameters.

weight of the water removed. For this estimation, it was considered that the environment inside the cloud chamber was saturated over water due to the presence of supercooled water droplets during the runs.

[13] A sample of the particles inside the cloud chamber (droplets and ice crystals) was collected on 2 mm wide glass strips, previously covered with a thin layer of a 5% wt/wt Formvar solution in chloroform [*Schaefer*, 1956]. The collection was made by pumping out a known air volume from the cloud chamber into the coated strip; then, the number concentrations and the sizes of the cloud droplets and ice crystals could be estimated. Figure 3 shows the box charts for the cloud droplet size distributions for $T = -8°C$, $-10°C$, and $-12°C$. The squares and horizontal bars inside the boxes give the mean and median droplet diameters, respectively. The boxes indicate the standard deviation, and the small dashes give the minimum and maximum droplet diameters. The sizes extend to 55 μm, and the average sizes are around 23 μm. The results show that the droplet size distributions were quite similar for the different temperatures used in this study.

[14] The following steps were followed to run an experiment:

[15] 1. The cold chamber was adjusted to the desired temperature.

[16] 2. The boiler introduced vapor for about 4 min. During this time, the droplets filled the cloud chamber and reached thermal equilibrium with the environment.

[17] 3. The ice crystals were nucleated, and the boiler continued introducing vapor up to the end of the run.

[18] 4. After nucleation, the ice crystals grew at the expense of the droplets in the chamber during 1 min.

[19] 5. The power to the air pump was switched on, and the graupel charging current was measured for a lapse of time between 40 and 50 s.

3. Results and Discussions

[20] The electrical charge separation was measured during collisions between ice crystals and the fixed target growing by riming (rimer). The experiments were carried out at around three ambient temperatures, namely $-8°C$, $-10°C$, and $-12°C$; impact velocities between 1 and 3 m s^{-1}; and effective liquid water content between 0.05 and 0.5 g m^{-3}. Figure 4 shows the diagrams of the sign of the charge to the target as a function of the ambient temperature and the effective liquid water content for three different velocities. This figure displays the experimental data and their associated error bars, showing the magnitudes of the uncertainties involved in the measurements. Dark circles indicate T-EW combinations for which the laboratory rimer charged negatively, and empty circles indicate positive charging of the rimer. Figures 4a–4c show the data corresponding to velocities of 1.8, 2.4, and 3.0 m s^{-1}, respectively. From Figure 4, the change of the positive and negative charging regions for the different velocities is clear. The results show that for $V = 1.8$ m s^{-1}, the target charges positively independently of the T and EW; while at higher velocities (2.4 and 3 m s^{-1}), a negative rimer charging zone appears at temperatures below $-10°C$ and EW < 0.2 g m^{-3}. At temperatures around $-8°C$, the target charges positively independently of the EW and V. Although the microphysical and environmental conditions are not completely analogous, these results can be compared with those reported by *Jayaratne et al*. [1983] and *Saunders et al*. [1991], who used a target of 5 mm in diameter and $V = 3$ m s^{-1}. These authors found negative charging of the rimer at temperatures above $-10°C$ and EW < 0.2 g m^{-3} and positive charging of the rimer at higher EW. The current data for $V = 3$ m s^{-1} (Figure 4c) show that the graupel charging is positive for temperatures above $-10°C$ and EW between 0.1 and 0.5 g m^{-3}. While at temperatures below $-10°C$, *Jayaratne et al*. [1983] and *Saunders et al*. [1991] found that the charging of the graupel has a similar behavior as those reported in the current work (Figure 4c). On the other hand, *Prakash and Kumar* [2010] found positive charging of the rimer for temperatures between $-7°C$ and $-12°C$, EW < 0.05 g m^{-3}, and $V = 2.2$ m s^{-1}.

[21] The average charge transferred to the riming target per rebounding ice crystal (q) can be estimated by using the equation

$$I = n \times p \times q, \tag{1}$$

where I is the charging current of the graupel; n is the number of ice crystals hitting the graupel per unit time; and p is the separation probability, defined as the probability that an ice crystal impacts and rebounds from the target. Only those ice crystals that collide and rebound are able to separate electric charge. For simplicity and because we lack more detailed information, we will assume that $p = 1$.

[22] The number of ice crystals hitting the graupel per unit time can be estimated from the equation

$$n = \mathrm{Ec} \times N \times V \times A, \tag{2}$$

where A is the cross-sectional area of the target; N is the ice crystal number concentration in the cloud; and Ec is the average collision efficiency of the target for ice crystals, defined as the proportion of crystals in the path of the collector, which actually collide with the collector. Assuming that the collision efficiencies of the target and the glass strips used as sampler are the same, then the factor Ec × N can be estimated from the formvar samples. It is worth to mention that the geometries of the collectors are not the same; then,

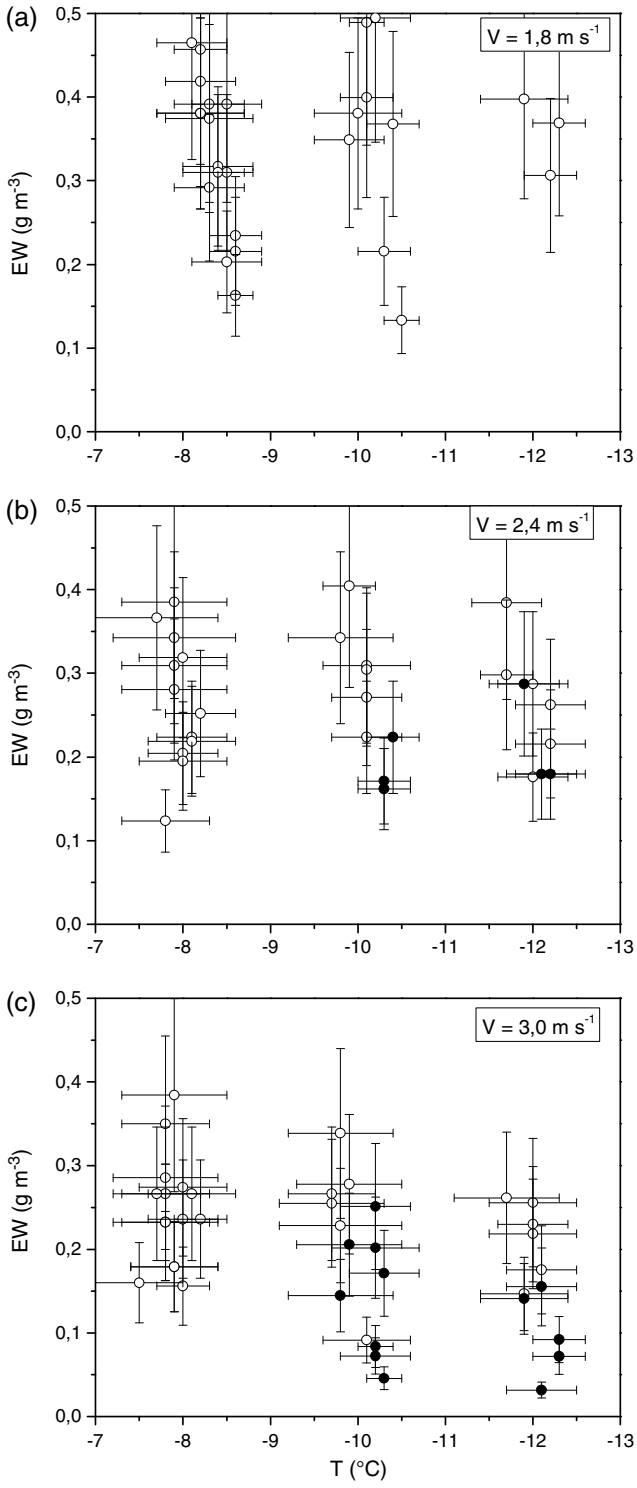

Figure 4. Experimental points of the rimer charge sign as a function of EW and T at three different velocities: (a) $1.8\,\mathrm{m\,s^{-1}}$, (b) $2.4\,\mathrm{m\,s^{-1}}$, and (c) $3.0\,\mathrm{m\,s^{-1}}$. Dark circles indicate negative charging of the rimer, and empty circles belong to positive results.

collisions efficiencies of the target and strips could be slightly different; however, we assume that this difference is insignificant.

[23] By using equations (1) and (2), the average charge transfer per collision can be obtained as

$$q = I(\mathrm{Ec} \times N \times V \times A)^{-1} \tag{3}$$

[24] Figure 5 displays the average charge transfer per collision as a function of the ice crystal mass for an ambient temperature of -8°C and a velocity of $3\,\mathrm{m\,s^{-1}}$ (Figure 5a) and for an ambient temperature of -10°C and a velocity of $2.4\,\mathrm{m\,s^{-1}}$ (Figure 5b). Although previous measurements use the particle size as a variable to characterize the average charge transfer per collision, in this work, the ice crystal mass was chosen as the variable because this parameter is linked to the kinetic energy of the impacting particle. Ice columns prevailed for ambient temperatures of -8°C and -10°C. In order to facilitate a comparison between different variables (size and volume), Figure 6 shows the maximum dimension of the ice columns (length) as a function of their volume. The significant dispersion observed in these data is a consequence of the different aspect ratios that present the ice columns. For temperatures around -12°C, a mix of ice crystal habits was present in each experiment; in fact, ice columns, plates, and triangles were observed on the formvar samples. Thus, the average crystal mass was obtained regarding the growth mode of the ice crystals [*Ono*, 1970], measuring the average sizes of each one of the crystal habits and taking into account the numeric proportion of each one of them.

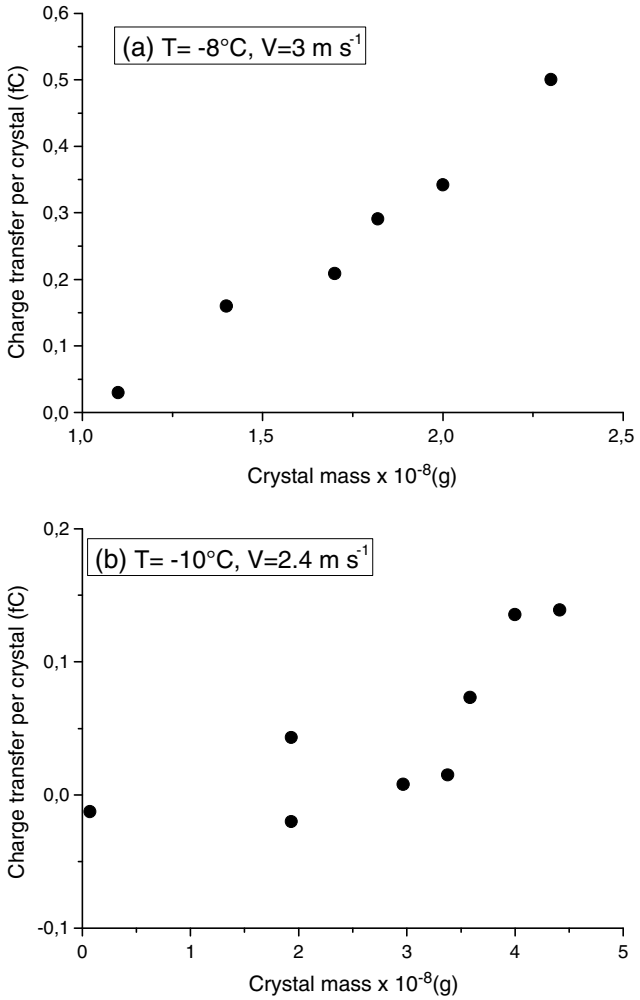

Figure 5. Average charge transferred as a function of ice crystal mass for (a) $T = -8$°C and $V = 3\,\mathrm{m\,s^{-1}}$ and (b) $T = -10$°C and $V = 2.4\,\mathrm{m\,s^{-1}}$.

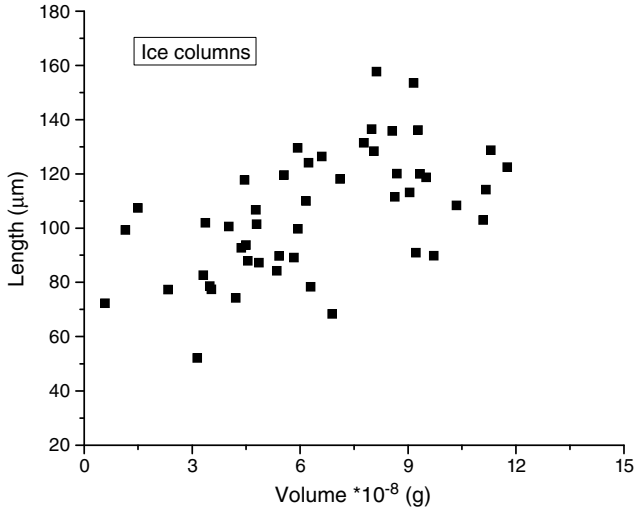

Figure 6. Ice columns length as a function of their volume, for temperatures of −8°C and −10°C.

[25] The magnitude of the average charge separated per collision is proportional to the average crystal mass. These results are consistent with results reported by other authors [*Jayaratne et al*., 1983; *Keith and Saunders*, 1989] who found that the charge transfer per collision is proportional to the size of the ice crystals. For instance, *Jayaratne et al*. [1983] found that the average charge increases with the ice crystal size for ice crystals between 20 and 100 μm, a temperature of −6°C, and a velocity of 2.8 m s^{-1}. They observed that the average charge was positive and varied between 0.01 and 1 fC, which is similar to the current results for $V = 3\ m\ s^{-1}$ and $T = -8°$ C (Figure 5a).

[26] The sign and magnitude of the charge transferred per collision as a function of the impact velocity is shown in Figure 7. These data were obtained for an ambient temperature of −8°C and an average crystal mass of 2×10^{-8} g (Figure 7a) and for an ambient temperature of −10°C and an average crystal mass of 4×10^{-8} g (Figure 7b). The charge per event was found to increase at higher impact speeds; this is also in agreement with the results reported by *Jayaratne et al*. [1983].

[27] The results clearly indicate that the magnitude of the average charge increases at warmer temperatures. Figure 8 shows the average charge transfer per collision as a function of the ice crystal mass for temperatures of −8°C and −10°C and a constant impact velocity of 2.4 m s^{-1}. The data show that under similar conditions of ice crystal size and impact velocity, the charge transferred to the graupel at −8°C is substantially larger than the average charge at −10°C.

[28] It is fair to remark that the supercooled water droplets and ice crystal concentrations and sizes change throughout an individual run, due to the mixed phase clouds that are thermodynamically unstable because of the difference of water vapor saturation over ice and liquid. We cannot know the temporal evolution of these variables because no more than one sample per run was taken. However, we observed that the charging currents of the graupel are relatively uniform throughout the measurements, indicating that these variations do not affect substantially the charge transfer processes.

[29] The reasons for the discrepancy between the current results and those from *Jayaratne et al*. [1983] and *Saunders et al*. [1991], particularly for temperatures above −10°C and EW < 0.2 g m^{-3}, are not completely understood. Both sets of experiments were performed in a single cloud chamber; however, the microphysical conditions were not the same. One important difference is that the graupel sizes were substantially different; it can produce accretions with different structures and ice densities under the same environmental conditions; it is expected that the smaller the size of the graupel, the lower the density of the accreted rime. *Williams and Zhang* [1996] proposed that the rime density may affect the charging behavior during ice particle collisions; in particular, they suggested that the rime with lower densities favors the positive charging. The other important variable in the laboratory simulations that affects the graupel charging is the supercooled cloud droplet size distribution. *Ávila et al*. [1999] showed that subtle differences in the droplet size distribution can produce changes in the sign of the rimer charging during ice-ice collisions. Differences in the cloud droplet spectra between both sets of experiments could be the reason of the discrepancy between the results; but not much information of the spectra was reported in the previous studies in order to evaluate possible differences. On the other hand, the

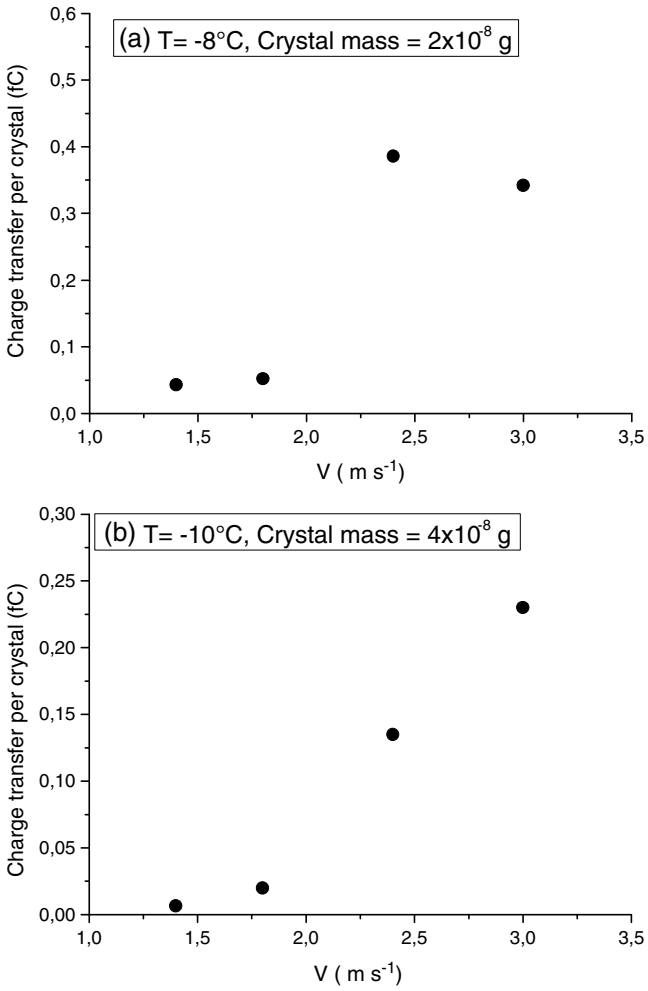

Figure 7. Average charge transferred as a function of the impact velocity for (a) $T = -8°C$ and an average crystal mass of 2×10^{-8} g and (b) $T = -10°C$ and an average crystal mass of 4×10^{-8} g.

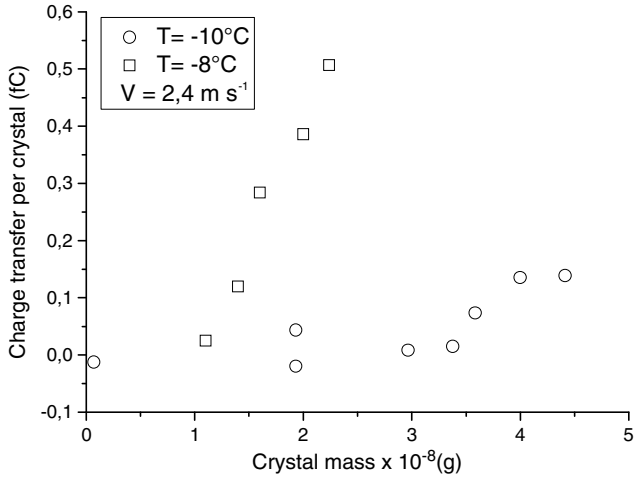

Figure 8. Average charge transferred per collision as a function of the ice crystal mass for temperatures of −8°C and −10°C and a constant $V = 2.4\ \mathrm{m\,s^{-1}}$.

polarity of the charge transfer in ice-particle collisions is determined by the state of growth of the interacting ice surfaces either by sublimation or deposition [*Saunders et al.*, 1991]. The ice surfaces grow or sublimate depending on the vapor pressure difference between the surfaces and the environment. In this context, the water vapor can be subsaturated or supersaturated with respect to water, and this may influence the sign of the separated charge. In general, the water vapor pressure is a variable which is usually not controlled during the experiments; thus, differences in the vapor pressures could be another possible reason of the inconsistency between the results of different measurements.

4. Effects on Cloud Electrification

[30] The stratiform regions of the MCS are generally associated with updraft speeds ~ $1\ \mathrm{m\,s^{-1}}$ and liquid water content $0.5\ \mathrm{g\,m^{-3}}$. They present a large concentration of small ice particles, graupel with sizes that ranged from 1 to 3 mm and fall speeds between 1 and $3\ \mathrm{m\,s^{-1}}$ [*Willis and Heymsfield*, 1989; *Schuur and Rutledge*, 2000].

[31] Based on the noninductive charging mechanism, *Williams and Yair* [2006] explained conceptually the lower positive charge layer in the stratiform regions of the MCS. They suggested that the characteristic low liquid water content promotes the positive charging of graupel particles. Thus, the positive charge is carried by falling graupel at lower levels (~ 0°C isotherm), and the negative charge is carried by the smaller ice particles at higher levels, leading to the typical inverted dipole structures in these clouds. The present results show that under conditions which resemble those available in the mesoscale updraft region of the MCS, the precipitation ice particles of millimeter size preferentially acquire a positive charge as a consequence of collisions with ice crystals. These results are in agreement with the model proposed by *Williams and Yair* [2006]. However, the application of these results is limited to the temperature range from −7°C to −13°C. Warmer temperatures were not explored in this study because of the difficulty of producing clouds with low liquid water content.

[32] It is important to note that the magnitude of the charge separated per individual collision is between 1 and 2 orders of magnitude smaller than the charge separation in convective thunderstorm conditions, which is around 10 fC [e.g., *Pereyra and Ávila*, 2002]. This is most probably a consequence of the low velocities involved in the collisions. However, we can conjecture that in principle, charge separation by individual collisions is a significant mechanism in the electrification processes of the stratiform regions of the MCS. This is so because even though the magnitude of the charge separation per collision is low, the residence time of the graupel in the stratiform regions may be longer than that in the convective regions. Thus, the mechanism of charge separation during ice crystal-graupel collisions is likely to contribute to the positive charge layers in this region and could be operating together with other mechanisms such as the melting charging.

[33] Considering the types of ice particles inside the mesoscale updraft regions of the MCS, it is important to mention that, likely, the collisions simulated in this study (graupel/pristine ice crystals) do not represent the collisions that mostly occur within these regions. In fact, frozen droplets and irregular aggregates are the most abundant small ice particles, and very few pristine crystals are observed.

5. Summary and Conclusion

[34] New laboratory measurements of the charge transfer in collisions between vapor-grown ice crystals and a target of 2 mm in diameter growing by riming are presented in this work. The experiments were conducted for ambient temperatures between −7°C and −13°C, air velocities between 1 and $3\ \mathrm{m\,s^{-1}}$, and effective liquid water content up to $0.5\ \mathrm{g\,m^{-3}}$, with the goal of studying the performance of the noninductive collisional charging of ice crystals and graupel mechanism under microphysical conditions similar to those found in stratiform cloud regions. The results from this work show the following:

[35] 1. The magnitude of the charge separation involved in the ice-ice collisions mechanism depends on the ice crystal mass, T, and velocity.

[36] 2. There is a positive charge transferred to the larger, faster falling particles at temperatures warmer than −10°C.

[37] 3. Negative graupel charging appears at low EW and temperatures below −10°C.

[38] 4. The magnitude of the charge transferred is between 1 and 2 orders of magnitude smaller than the charge separation in convective thunderstorm conditions. This is probably a consequence of the low velocities involved in the collisions.

[39] Finally, we can conclude that the mechanism of charge separation during ice crystal-graupel collisions could, in principle, contribute to the electrification processes in the mesoscale updraft region of the MCS, provided that the residence time of the graupel in the cloud is sufficiently long.

[40] **Acknowledgments.** This work was supported by Secretaria de Ciencia y Tecnología de la Universidad Nacional de Córdoba, Consejo Nacional de Investigaciones Científicas y Tecnológicas (CONICET), and Agencia Nacional de Promoción Científica (FONCYT). We want to thank Jose Barcelona for his technical assistance.

References

Ávila, E. E., and R. G. Pereyra (2000), Charge transfer during crystal-graupel collisions for two different cloud droplet size distributions, *Geophys. Res. Lett.*, *27*(23), 3837–3840.

Ávila, E. E., R. G. Pereyra, G. G. Aguirre Varela, and J. M. Caranti (1999), The effect of the cloud droplet spectrum on electrical charge transfer during individual ice-ice collisions, *Q. J. R. Meteorol. Soc.*, *125*, 1669–1679.

Boccippio, D. J., E. R. Williams, S. J. Heckman, W. A. Lyons, I. T. Baker, and B. Boldi (1995), Sprites, ELF transients and positive ground strokes, *Science*, *269*, 1088–1091.

Brooks, I. M., C. P. R. Saunders, R. P. Mitzeva, and S. L. Peck (1997), The effect on thunderstorm charging of the rate of rime accretion by graupel, *Atmos. Res.*, *43*, 277–295.

Bürgesser, R. E., R. G. Pereyra, and E. E. Ávila (2006), Charge separation in updraft of convective regions of thunderstorm, *Geophys. Res. Lett.*, *33*, L03808, doi:10.1029/2005GL023993.

Fabry, F., and I. Zawadzki (1995), Long-term radar observations of the melting layer of precipitation and their interpretation, *J. Atmos. Sci.*, *52*, 838–851.

Jayaratne, E. R., C. P. R. Saunders, and J. Hallett (1983), Laboratory studies of the charging of soft hail during ice crystal interactions, *Q. J. R. Meteorol. Soc.*, *109*, 609–630.

Keith, W. D., and C. P. R. Saunders (1989), Charge transfer during multiple large ice crystal interactions with a riming target, *J. Geophys. Res.*, *94*, 13,103–13,106.

Lighezzolo, R. A., R. G. Pereyra, and E. E. Avila (2010), Measurements of electric charge separated during the formation of rime by the accretion of supercooled droplets, *Atmos. Chem. Phys.*, *10*, 1661–1669.

Locatelli, J. D., and P. V. Hobbs (1974), Fall speeds and masses of solid precipitation particles, *J. Geophys. Res.*, *79*(15), 2185–2197, doi:10.1029/JC079i015p02185.

Lyons, W. (1996), Sprite observations above the U.S. High Plains in relation to their parent thunderstorm systems, *J. Geophys. Res.*, *101*, 29,641–29,652.

Marshall, T. C., and W. D. Rust (1993), Two types of vertical electrical structures in stratiform precipitation regions of mesoscale convective systems, *Bull. Am. Meteorol. Soc.*, *74*, 2159–2170.

Ono, A. (1970), Growth mode of ice crystals in natural clouds, *J. Atmos. Sci.*, *27*, 649–658.

Pereyra, R. G., and E. E. Ávila (2002), Charge transfer measurements during single ice crystal collisions with a target growing by riming, *J. Geophys. Res.*, *107*(D23), 4735, doi:10.1029/2001JD001279.

Pereyra, R. G., E. E. Ávila, N. E. Castellano, and C. P. R. Saunders (2000), A laboratory study of graupel charging, *J. Geophys. Res.*, *105*, 20,803–20,813.

Pereyra, R. G., R. E. Bürgesser, and E. E. Ávila (2008), Charge separation in thunderstorm conditions, *J. Geophys. Res.*, *113*, D17203, doi:10.1029/2007JD009720.

Prakash, P. J., and P. P. Kumar (2010), Effect of sulfates and chlorides on electrification by a noninductive process applicable to stratiform clouds, *J. Geophys. Res.*, *115*, D02206, doi:10.1029/2009JD012470.

Reynolds, S. E., M. Brook, and M. F. Gourley (1957), Thunderstorm charge separation, *J. Meteorol.*, *14*, 426–436.

Saunders, C. P. R., and S. L. Peck (1998), Laboratory studies of the influence of the rime accretion rate on charge transfer during crystals/graupel collisions, *J. Geophys. Res.*, *103*, 13,949–13,956.

Saunders, C. P. R., W. D. Keith, and R. P. Mitzeva (1991), The effect of liquid water on thunderstorm charging, *J. Geophys. Res.*, *96*, 11,007–11,017.

Saunders, C. P. R., E. E. Avila, S. L. Peck, N. E. Castellano, and G. G. Aguirre Varela (1999), A laboratory study of the effects of rime ice accretion and heating on charge transfer during ice crystal/graupel collisions, *Atmos. Res.*, *51*, 99–117.

Saunders, C. P. R., S. L. Peck, G. G. Aguirre Varela, E. E. Avila, and N. E. Castellano (2001), A laboratory study of the influence of the water vapour and mixing on the charge transfer process during collisions between ice crystals and graupel, *Atmos. Res.*, *58*, 187–203.

Saunders, C. P. R., H. Bax-Norman, E. E. Avila, and N. E. Castellano (2004), A laboratory study of the influence of ice crystal growth conditions on subsequent charge transfer in thunderstorm electrification, *Q. J. R. Meteorol. Soc.*, *130/B*, 1395–1406.

Saunders, C. P. R., H. Bax-Norman, C. Emersic, E. E. Avila, and N. E. Castellano (2006), Laboratory studies of the effect of cloud conditions on graupel/crystal charge transfer in thunderstorm electrification, *Q. J. R. Meteorol. Soc.*, *132/B*, 2655–2676.

Schaefer, V. J. (1956), The preparation of snow crystal replicas—VI, *Weatherwise*, *9*, 132–135, doi:10.1080/00431672.1956.9927220.

Schuur, T. J., and S. A. Rutledge (2000), Electrification of stratiform regions in mesoscale convective systems. Part I: An observational comparison of symmetric and asymmetric MCSs, *J. Atmos. Sci.*, *57*, 1961–1982.

Schuur, T. J., B. F. Smull, W. D. Rust, T. C. Marshall (1991), Electrical and kinematic structure of the stratiform precipitation region trailing an Oklahoma squall line, *J. Atmos. Sci.*, *48*, 825–842.

Shepherd, T. R., W. D. Rust, and T. C. Marshall (1996), Electric fields and charges near 0°C in stratiform clouds, *Mon. Weather Rev.*, *124*, 919–938 , doi:10.1175/1520-0493.

Stolzenburg, M., and T. C. Marshall (2008), Charge structure and dynamics in thunderstorms, *Space Sci. Rev.*, *137*, 355–372, doi:10.1007/s11214-008-9338-z.

Stolzenburg, M., T. C. Marshall, W. D. Rust, and B. F. Smull (1994), Horizontal distribution of electrical and meteorological conditions across the stratiform region of a mesoscale convective system, *Mon. Weather Rev.*, *122*, 1777–1797.

Stolzenburg, M., W. D. Rust, B. F. Smull, and T. C. Marshall (1998), Electrical structure in thunderstorm convective regions: 1. Mesoscale convective systems, *J. Geophys. Res.*, *103*, 14,059–14,078, doi:10.1029/97JD03546.

Takahashi, T. (1978), Riming electrification as a charge generating mechanism in thunderstorms, *J. Atmos. Sci.*, *35*, 1536–1548.

Williams, E. (1998), The positive charge reservoir for sprite-producing lightning, *J. Atmos. Sol. Terr. Phys.*, *60*, 689–692.

Williams, E. R., and Y. Yair (2006), The microphysical and electrical properties of sprite producing thunderstorms, in *Sprites, Elves and Intense Lightning Discharges*, NATO Sci. Ser. II, Math., Phys. and Chem., vol. *225*, 57–83 pp., edited by M. Füllekrug, E. A. Mareev, and M. J. Rycroft, Springer, Dordrecht, The Netherlands.

Williams, E., and R. Zhang (1996), Density of rime in laboratory simulations of thunderstorm microphysics and electrification, *J. Geophys. Res.*, *101*, 29,715–29719.

Willis, P. T., and A. J. Heymsfield (1989), Structure of the melting layer in mesoscale convective system stratiform precipitation, *J. Atmos. Sci.*, *46*, 2008–2025.